The Journal of Engineering

The 7th International Conference on Renewable Power Generation (RPG 2018)

Reducing voltage fluctuations using DSTATCOMs and reactive power of PV inverters in a medium voltage distribution system

eISSN 2051-3305
Received on 26th October 2018
Accepted on 10th January 2019
E-First on 18th June 2019
doi: 10.1049/joe.2018.9279
www.ietdl.org

Duong Quoc Hung[1] ✉, Yateendra Mishra[1], Geoffrey Walker[1]
[1]*School of Electrical Engineering and Computer Science, Queensland University of Technology, Brisbane, Queensland 4000, Australia*
✉ *E-mail: hung.duong@qut.edu.au*

Abstract: This paper proposes local reactive power control to mitigate the voltage fluctuation in medium-voltage systems using DSTATCOMs and photovoltaic (PV) inverters. New expressions are developed to estimate voltage fluctuations and reactive power compensations by transforming line segment power-flow variables into nodal power injections. Using local measurements of voltages and solar powers, the method can provide a fast estimation of reactive power compensations to maintain the voltage at every bus. DSTATCOMs are also properly allocated to enhance the voltage controllability. Coordinated control of multiple reactive power resources is investigated as well. One-second solar irradiance along with one-minute home loads is used to demonstrate the effectiveness of the proposed method.

1 Introduction

The growing participation of PV generators in distribution systems has raised immediate concerns about voltage security [1–3]. The rapid voltage rise due to fast cloud movements from a few seconds to minutes has been reported on distribution feeders during daytime. Meanwhile, the sharp voltage drop due to the contribution of heavy loads, including home charging for electric vehicles has been observed at night-time [4]. It, therefore, becomes particularly essential to develop an efficient reactive power compensation solution to mitigating the voltage fluctuation in the distribution grid.

Voltage regulators and switchable capacitors are traditionally designed to mitigate slow voltage fluctuations due to load variability. On the other hand, future reactive power control must deal with rapid and random voltage fluctuations due to the acceleration of PV penetration [3, 5]. Particularly, PV inverters can offer a fast reactive power response to eliminating such voltage fluctuations in addition to energy provision as the primary task under the standard IEEE 1547 in [6]. However, more costly oversized PV inverters are required and PV inverters to control reactive power can reduce the capability of solar energy harvest. This issue, therefore, might be one of the major challenges to motivate PV owners to support daytime voltage regulation in [7]. In addition, reactive power injections by PV inverters are not prevalently accepted by almost all utilities in [3] or possibly restricted by a 0.95 or 0.9 leading/lagging power factor capability [8, 9]. Further research into nighttime PV inverters operation are still necessary in [10]. Unlike PV inverters, distribution static synchronous compensators (DSTATCOMs) can be used as an independent reactive power source for voltage regulation. Hence, the current paper deploys DSTATCOMs to maintain the voltage while PV inverters are fully utilised to harvest solar energy during daytime. At night-time, PV inverters are used to reduce the capability of DSTATCOMs.

An enormous number of publications have developed control methods to address the voltage rise issue. Given full-network information, centralised reactive power control was formulated as an optimal power flow (OPF) solution to reduce system operational costs such as voltage deviations and power losses in [11, 12]. Voltage sensitivity analyses with respect to nodal power variations were made on the basis of a Jacobian matrix generated by Newton Raphson power-flows, as an efficient voltage control measure in [1, 2, 13, 14]. Yet, the sensitivities are necessarily updated according to the time-variability of loads and generation that requires full-network measurements as well in [15]. Similarly, variable power factor and active power sensitivity methods were introduced to control reactive power provided by PV farms in [7]. A gradient-projection method offered local voltage control to reduce the voltage fluctuation generated by fast cloud movements in [16], but ignored coordination among multiple reactive power facilities. In [15], a surface-fitting technique was adopted to capture voltage sensitivities according to variations of nodal active reactive power injections based on local-wind plants' observability. This solution, nonetheless, was limited to single-plant control. Hence, time-delays were employed to take coordinated control actions of multiple plants in a sequential manner to prevent over-compensation. Similarly, time-delays were adopted to control multiple reactive power resources in [3]. However, time-delays would not provide a simultaneous response to the rapid voltage rise detected by various reactive power devices on the same feeder.

This paper presents fast local reactive power control to reduce the voltage fluctuation in medium-voltage systems. New expressions are developed based on transforming line segment power-flow variables into nodal power injections to estimate voltage fluctuations and local reactive power compensations at each bus. A DSTATCOM allocation algorithm is then presented to enhance the voltage controllability for the entire system. Coordinated control of multiple reactive power resources, including DSTATCOMs and PV inverters is investigated in the paper as well.

The rest of this paper is organised as follows: Section 2 presents its methodology. Section 3 shows results obtained on an 18-bus distribution feeder. Finally, the contributions and conclusion of the work are briefly described in Section 4.

2 Methodology

2.1 Background

2.1.1 Distribution system model: Consider a distribution system with n buses in Fig. 1. Its power flows can be described by the linearised *LineDistFlow* in [5, 17]:

$$P_{i+1} = P_i - P_{Li+1} + p_{Gi+1} \tag{1}$$

$$Q_{i+1} = Q_i - q_{Li+1} + q_{Gi+1} \tag{2}$$

$$\Delta V_{i+1} = V_i - V_{i+1} \frac{r_i P_i + x_i Q_i}{V_1} \quad (3)$$

$$P_{Gi+1} = P_{PVi+1}; q_{Gi+1} = q_{PVi+1} + q_{\text{DSTATCOM}i+1} \quad (4)$$

where P_i and Q_i denote the active and reactive powers across line segment *i*, respectively; p_{Li+1} and q_{Li+1} are the active and reactive power loads at bus $i+1$, respectively; p_{Gi+1} and q_{Gi+1} are the active and reactive powers of the power electronic device (ED)-based generator at bus $i+1$, including a PV inverter and a DSTATCOM; r_i and x_i are the line segment impedance from bus i to bus $i+1$; V_1 is the reference voltage at the substation and V_i is the voltage at bus i; $q_{\text{DSTATCOM}i}$ is the reactive power rating of the DSTATCOM at bus i; p_{PVi+1} and q_{PVi+1} are the active power output of the PV module at bus $i+1$, respectively. Theoretically, DSTATCOMs are modelled as a reactive power resource that is capable of controlling capacitive or inductive reactive power independently. Unlike DSTATCOMs, PV generators typically consist of PV modules and associated inverters.

These PV inverters are allowed to inject or absorb a limited amount of reactive power to support the grid in addition to energy provision in [6, 8, 9]. To avoid lowering the active power output of PV modules, the maximum reactive power of the inverter is limited by the active power output of PV modules, as follows:

$$q_{PVi+1} = \sqrt{s_{PVi+1}^2 - p_{PVi+1}^2} \quad (5)$$

Where s_{PVi+1} denotes the apparent power rating of the PV inverter at bus $i+1$.

2.1.2 Centralised versus local control: The voltage fluctuation across a line segment between buses i and $i+1$ of the feeder is derived from (3) as [5, 17]:

$$\Delta V_{i+1}(P_i, Q_i, P_{Gi+1}, q_{Gi+1}) = \frac{r_i(P_i - P_{Gi+1}) + X_i(Q_i - q_{Gi+1})}{V_1} \quad (6)$$

To calculate the voltage at each bus, (6) updates global variables of line segment power-flows (i.e., P_i and Q_i) every time according to changes in power injections. More specifically, the voltage fluctuation through a segment between buses i and $i+1$ hinges on the power-flows across that segment. Given an active power injection at each bus (i.e., q_{Gi+1}), an optimisation-based centralised controller could estimate a sufficient amount of reactive power, q_{Gi+1} to minimise the voltage fluctuation, ΔV_{i+1}. This centralised control is quite contingent on the availability of communications, which are not yet common in distribution systems [15]. In addition, due to centralised control based on optimisation, potential network vulnerability such as communication delays or noises would challenge its optimality and stability for real-time applications [5, 16]. Unlike centralised control, a local control method can measure local variables of the voltage and PV power injection at each bus to calculate reactive power compensations. This solution can be solved in the current paper by transforming the global variables of line segment power-flows in (6) into local power injection variables, as detailed below.

2.2 Proposed local reactive power control

The voltage fluctuation across the distribution feeder with k buses, indexed by $i = 1, 2, \ldots, k$ is derived from (6) as

$$\Delta V_k = V_1 - V_k = \sum_{i=1}^{k} \frac{r_i P_i + X_i Q_i}{V_1}. \quad (7)$$

Due to the reactive power injection by the generator at bus k (or $i+1$), (7) can be modified as

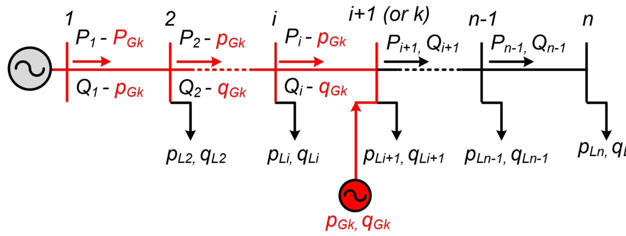

Fig. 1 *A distribution feeder with a generator*

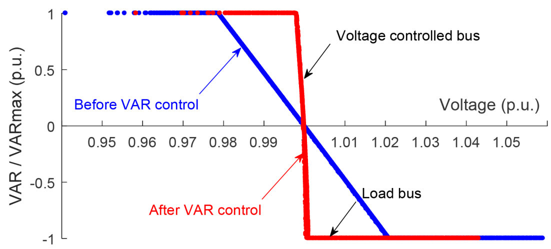

Fig. 2 *A Q-V curve at any bus in a feeder with VAR control*

$$\Delta V_{Gk} = V_1 - V_k = \sum_{i=1}^{k} \frac{r_i P_i - P_{Gk}}{V_1} + \sum_{i=1}^{k} \frac{X_i(Q_i - q_{Gk})}{V_1}. \quad (8)$$

Equation (8) can be re-arranged as

$$\Delta V_{Gk}(\Delta V_k, p_{Gk}, q_{Gk}) = \Delta V_k - \sum_{i=1}^{k} \frac{r_i P_{Gk} + X_i q_{Gk}}{V_1}. \quad (9)$$

It is observed that instead of using line segment power-flows as expressed in (6), (9) can measure local information (i.e., ΔV_k, p_{Gk} and q_{Gk}) to calculate the voltage fluctuation at each bus. In this regard, the local reactive power controlled at bus k can be derived from (9) given $\Delta V_{Gk} = V_1 - V_{Gk}$, as follows:

$$q_{Gk}(\Delta V_k, p_{Gk}) = \frac{V_{Gk} - V_1 + \Delta V_k - \sum_{i=1}^{k} r_i p_{Gk}/V_1}{\sum_{i=1}^{k} X_i/V_1} \quad (10)$$

where V_{Gk} is the voltage after reactive power compensation at bus k. Equation (10) is a function of local variables, ΔV_k and p_{Gk}. To control the voltage at the connection point of an ED at bus k, the voltage at that bus is treated as the setpoint voltage (i.e., $V_{Gk} = V_{SPk}$, 1 p.u.). This bus is referred to as a voltage-controlled bus. In practice, EDs are normally allowed to produce a limited amount of reactive power given by (11). Hence, during the calculation process, if the reactive power limit of any ED is violated, its output is fixed at the given limit, and the corresponding voltage-controlled bus is treated as a PQ or load bus.

$$-q_{Gk}^{\max} \le q_{Gk} \le q_{Gk}^{\max}. \quad (11)$$

As an example, Fig. 2 shows a typical reactive power-voltage control (Q-V) curve at a bus in a distribution feeder with PV generators. This pattern is generated by (9)-(11) using the data of an 18-bus feeder associated with load and PV profiles detailed in Section 3. The voltage can maintain at 1 p.u. when the reactive power (VAR) support by an ED is sufficient (i.e., voltage controlled-bus). However, it is different from 1 p.u. (i.e., load bus) when the VAR required from the grid is larger than the maximum limit of the ED. It is worth mentioning that (9)-(11) can generate a similar Q-V curve as compared to the controller proposed in [18].

2.2.1 DSTATCOM allocation: To enhance local voltage controllability, an algorithm is proposed to accommodate DSTATCOMs into a distribution system so that the average voltage fluctuation for the entire system is minimised.

Algorithm 1: Allocation and sizing of DSTATCOMs

Step 1. Set the setpoint voltage, V_{SPk} for a given DSTATCOM.
Step 2. Estimate the amount of reactive power support at bus k by a DSTATCOM over time-period t from (10) with $V_{Gk} = V_{SPk}$.

$$q_{Gk,t}(\Delta V_{k,t}, p_{Gk,t}) = \frac{V_{SPk} - V_1 + \Delta V_{k,t} - \sum_{i=1}^{k} r_i p_{Gk,t}/V_1}{\sum_{i=1}^{k} x_i/V_1} \tag{12}$$

Step 3. Update the voltage fluctuation at each bus over time period t from (9) and (12):

$$\Delta V_{Gk,t}(\Delta V_{k,t}, p_{Gk,t}, q_{Gk,t}) = \Delta V_{k,t} - \sum_{i=1}^{k} \frac{r_i p_{Gk,t} + x_i q_{Gk,t}}{V_1}. \tag{13}$$

Step 4. Estimate the average voltage fluctuation factor in percent for the feeder as below, where Ns is the number of PV output states.

$$\%AVFF = \frac{100}{Nb \times Ns} \sum_{i=1}^{Nb} \sum_{t=1}^{Ns} |\Delta V_{Gk,t}|. \tag{14}$$

Step 5. Locate the best location where the *%AVVF* is lowest with the corresponding size at that location.

2.2.2 Coordinated reactive power control:

To take multiple ED control actions simultaneously, an algorithm for controlling multiple EDs is described below.

Algorithm 2: Coordinated reactive power control

Step 1. Set the setpoint voltages for all given EDs.
Step 2. Estimate the amounts of reactive power support by multiple EDs over time-period t using (12).
Step 3. Calculate the summation of the reactive power provided by all the EDs involved over time period t
as below, where NG is the number of EDs.

$$\mathrm{SUM}_t = \sum_{k=1}^{NG} q_{Gk,t}. \tag{15}$$

Step 4. Determine the weighting factor assigned to each ED over time period t, as follows:

$$WF_{k,t} = \frac{q_{Gk,t}}{\mathrm{SUM}_t}. \tag{16}$$

Step 5. Update the reactive power support of each ED, from (12) and (16) over time period t as

$$q_{Gk,t}^{\mathrm{update}} = WF_{k,t} \times q_{Gk,t}. \tag{17}$$

Step 6. Update the voltage fluctuation at each bus over time period t using (13),
Step 7. Estimate the voltage fluctuation factor in percent as

$$\%VFF_{Gk,t} = 100 \times |\Delta V_{Gk,t}|. \tag{18}$$

3 Simulation results

The proposed method is applied to an 18-bus feeder extracted from the 12.7 kV IEEE 33-bus test system [17]. The demand of each feeder is assumed to follow a typical one-minute home load in [19], each of which accommodates a PV penetration level of 40%. The PV power output is converted from one-second solar irradiance data using the PV model and its parameters in [20, 21]. The load and PV output of the entire system are plotted in Fig. 3. To mitigate the fast voltage fluctuation due to the intermittency of PV output, this study takes the rating of existing customers' PV inverters and utility's DSTATCOMs capacity into consideration. In this regard, following assumptions are made in the simulation:

- During daytime, DSTATCOMs are utilised to eliminate the voltage fluctuations while PV inverters are fully used as negative loads to harvest the solar energy.

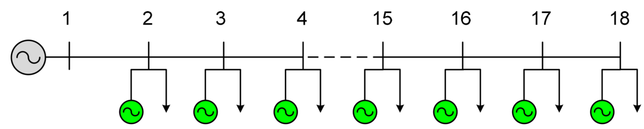

Fig. 3 *The 18-bus test feeder with PV generators*

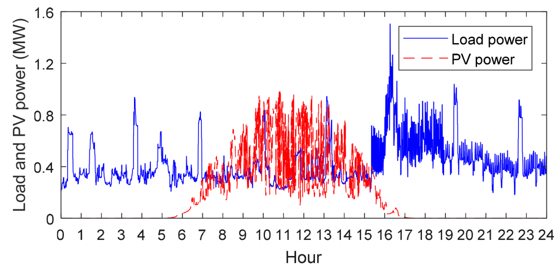

Fig. 4 *One-minute home load and PV output over a 24-h day*

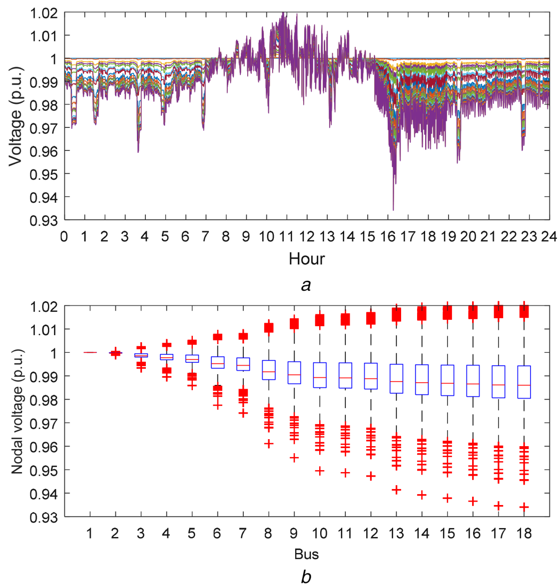

Fig. 5 *The base case feeder before VAR support over a 24-h day*
(a) Voltage profiles, and ***(b)*** Voltage boxplot

- At night-time, PV inverters are employed to reduce the reactive power capability of DSTATCOMs.

Due to fast cloud movements along with sharp demand variability, the whole system incurred a significant PV power fluctuation illustrated in Fig. 4. The resulting voltage fluctuations were considerable as described in Fig. 5*a*. Particularly, the time-variability of combined load-generation produced sharp voltage drops and rises with one-second resolution during the daytime, while voltage drops with one-minute resolution under the heavy load conditions occurred at the nighttime. From this calculated data, Fig. 5*b* represents the box plot of the voltages at various buses over the analysed day. Each box shows the central mark, bottom and top edges, respectively indicating the median, 25% percentile and 75% percentile, and outliers of the estimated data. It is observed from Fig. 5*b* that significant voltage drops and rises are observed at the end of the feeder, especially buses 16–18.

3.1 DSTATCOM allocation

Fig. 6 plots the average voltage fluctuation after reactive power support (*%AVFF*) over the day with respect to optimal sizes of DSTATCOMs accommodated at various buses of the feeder. Each optimal size is estimated as the maximum magnitude of the reactive power output absorbed by that DSTATCOM. The size varies significantly in the range of 1.36 to 0.33 MVar. The best location is found at bus 13, where the DSTATCOM is rated at 0.50 MVar. This size generates the lowest *%AVFF* value of 0.09. It is

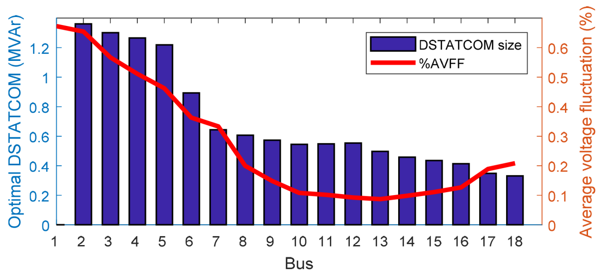

Fig. 6. *Optimal DSTATCOM size with respect to average voltage fluctuation factors at various locations*

Table 1 DSTATCOM allocation and corresponding *%AVFF*s

Methods	Bus	Size (MVar)	%AVFF	Required information
base case – No VAR	—	—	0.67	Local *Vk*
OPF-based VAR	13	0.51	0.09	Full-network
proposed VAR	13	0.50	0.09	Local *Vk*, *pGk*

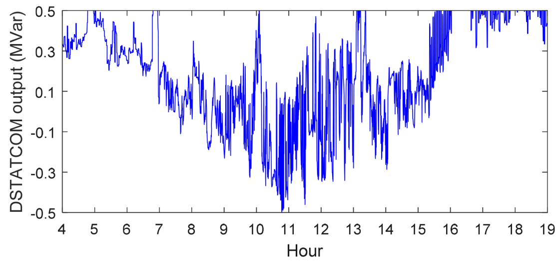

Fig. 7 *Daytime DSTATCOM control at bus 13*

also observed that the size estimated at bus 13 is significantly lower than the value at bus 5 as an example, which is 1.22 MVar with a *%AVFF* of 0.46. This indicates that the best solution requires a considerably lower amount of reactive power provided by DSTATCOMs while increasing the voltage controllability for the whole system. If the DSTATCOM is placed at the end of the feeder – bus 18, the optimal size further is reduced but the *%AVFF* is approximately doubled.

Table 1 shows a comparison of the results obtained from the proposed method and the optimal power flow (OPF) solution that is developed based on the Matpower software. The average voltage fluctuation (*%AVFF*) in the feeder after VAR support is reduced significantly in relation to the *%AVFF* in the original feeder before VAR support. It is worth mentioning that the proposed method using limited local measurements (i.e., V_k and $p_{Gk)}$ produces a rather similar outcome as compared to the OPF solution requiring full-network information.

3.2 Coordinated reactive power control

The DSTATCOM is intended to absorb the reactive power from the grid to eliminate the sharp voltage rise caused by the intermittency of PV generation. Meanwhile, it also injects the reactive power to reduce the voltage drop due to heavy loading. Fig. 7 depicts the daytime reactive power outputs of the DSTATCOM at bus 13 over every one-second resolution. The positive (+) and negative (−) signs respectively indicate that the DSTATCOM injects and absorbs the reactive power. The DSTATCOM offers a good response to the PV output fluctuations with one-second resolution in Fig. 4.

Figs. 8*a* and *b* represent the coordinated one-minute resolution control of multiple reactive power resources at all the buses connected with PV generators, from 0:00 to 4:00 and 19:00 to 24:00, respectively. It is observed that all the PV inverters at all the buses including the DSTATCOM at bus 13 participate in their reactive power support to the grid following the changes in the load demand. Some of the PV inverters offer a reactive power response

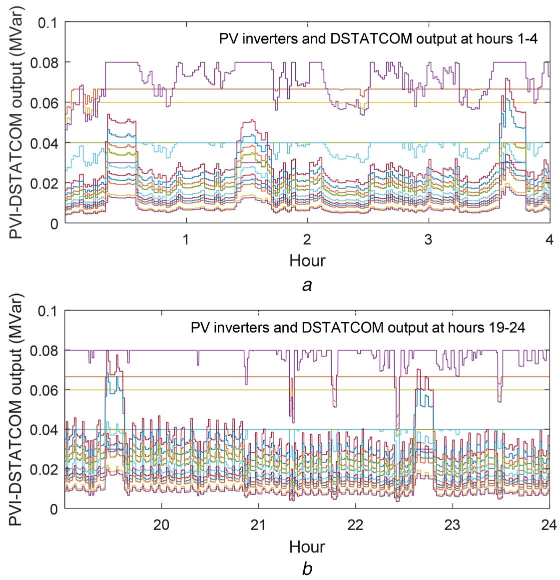

Fig. 8 *Night-time PV inverters control at all buses and DSTATCOM at bus 13*
(a) hours 1-4, and ***(b)*** hours 20–24

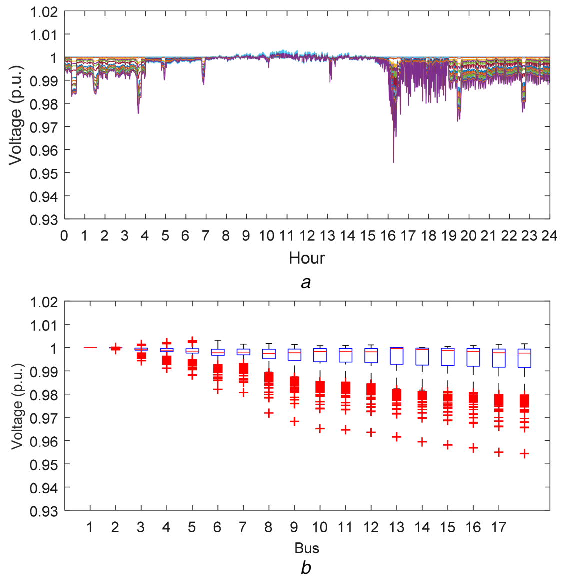

Fig. 9 *The feeder after VAR support over a 24-h day*
(a) Voltage profiles, and ***(b)*** Voltage boxplot

to the variations of the load demand. On the other hand, a few produce constant reactive powers at their ratings as the reactive powers required from the grid are larger than the maximum reactive powers supplied by PV inverters. The participation of all the PV inverters in the nighttime reactive power control enhances the voltage profiles for the whole feeder, as detailed in Fig. 9*a* and *b*.

Fig. 9*a* shows the results obtained by the proposed method at all the buses of the feeder over 24 h. With reactive power support by the PV inverters and DSTATCOMs, the voltage profile of the whole feeder is improved significantly. The voltage fluctuations in the feeder is reduced by approximately 2% as compared to the feeder without reactive power support described in Fig. 5*a*. Particularly, the voltage rise caused by the PV power output at all the buses over 24 h are nearly eliminated as shown in Fig. 9*b*.

Fig. 10 shows a cumulative distribution function (CDF) curve, which is generated from the voltage data analysed in Fig. 9*a*. The CDF curve represents the percentage of voltage fluctuations (*%VFF*) at every bus on the feeder over the analysed day. It is worth mentioning that the coordinated control of the PV inverters and DSTATCOM, referred to as PVI-DSTATCOM, produces the highest *%VFF* at almost every confidence level in relation to other

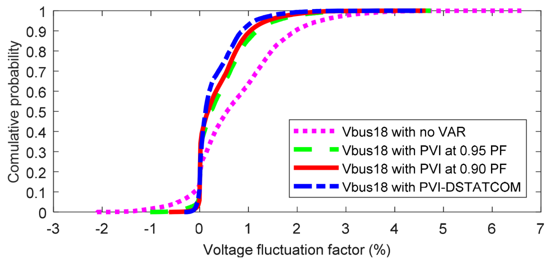

Fig. 10 *Voltage fluctuation CDFs by various VAR control solutions over a 24-h day*

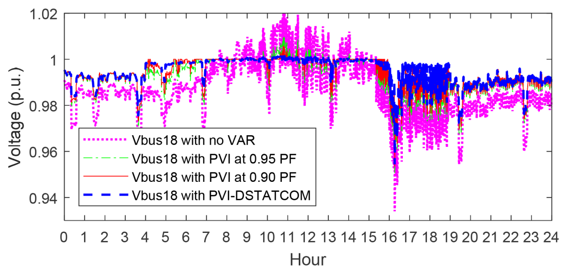

Fig. 11 *Voltage profiles at the end of the feeder (bus 18) with various VAR control solutions over a 24-h day*

Table 2 Maximum total generated power of PV inverters and corresponding *%AVFF*s by various VAR control solutions

Local VAR control solutions	Max. PV power	*%AVFF*	*%AVFF*
base case – No VAR	1.00	0.87	—
PVI at 0.95 power factor in [8]	0.95	0.46	47.13
PVI at 0.90 power factor in [9]	0.90	0.39	55.17
PVI-DSTATCOM (proposed)	1.00	0.32	63.22

three scenarios. These include no VAR control (i.e., base case system), and PV inverters (PVI) control at a 0.95 or 0.9 leading/lagging power factor in [8, 9]. Fig. 11 further plots the voltage profiles at the end of the feeder, where the worst voltages are observed for the all the scenarios. A significant voltage improvement is achieved for the scenario that includes the DSTATCOM in coordination with all the PV generators.

Table 2 summaries the average voltage fluctuations (*%AVFFs*) with respect to the maximum ratings of PV and corresponding VAR control. Inclusion of the DSTATCOM in the system reduces the voltage fluctuation significantly while maximising the solar power harvest. In contrast, higher voltage fluctuations along with less solar power harvest are obtained for the scenarios based on control of PV inverters only.

4 Conclusion

This paper presented fast local reactive power control to mitigate the voltage fluctuation caused by the intermittency of solar power in residential distribution systems. Using local measurements of voltages and solar power injections, the method can provide a quick estimation of voltage fluctuations and reactive power compensations at each bus. A DSTATCOM allocation algorithm was introduced to enhance the voltage controllability for the entire system. Coordinated control of multiple reactive power resources was investigated to reduce voltage fluctuations over a 24-h day. Numerical results confirm that the local control method produces an outcome similar to an OPF solution that requires full-network information. Inclusion of DSTATCOMs as an independent source in daytime control leads to a significant improvement on voltage profiles while maximising solar energy harvest. Meanwhile, coordinated control of multiple PV inverters makes a significant contribution to reduced voltage drops at night-time. Using limited local-network data, the proposed method can be a useful tool for real-time applications.

5 References

[1] Malekpour, A.R., Pahwa, A.: 'A dynamic operational scheme for residential PV smart inverters', *IEEE Trans. Smart Grid*, 2017, **8**, pp. 1–10

[2] Kabir, M.N., Mishra, Y., Ledwich, G., *et al.*: 'Coordinated control of grid-connected photovoltaic reactive power and battery energy storage systems to improve the voltage profile of a residential distribution feeder', *IEEE Trans. Ind. Informat.*, 2014, **10**, pp. 967–977

[3] Wang, Z., Chen, H., Wang, J., *et al.*: 'Inverter-less hybrid voltage/var control for distribution circuits with photovoltaic generators', *IEEE Trans. Smart Grid*, 2014, **5**, pp. 2718–2728

[4] Richardson, P., Flynn, D., Keane, A.: 'Optimal charging of electric vehicles in low-voltage distribution systems', *IEEE Trans. Power Syst.*, 2012, **27**, pp. 268–279

[5] Turitsyn, K., Sulc, P., Backhaus, S., *et al.*: 'Options for control of reactive power by distributed photovoltaic generators', *Proc. IEEE*, 2011, **99**, pp. 1063–1073

[6] 'IEEE standard for interconnecting distributed resources with electric power systems – amendment 1', IEEE Std 1547a-2014 (Amendment to IEEE Std 1547-2003), pp. 1–16 (2014).

[7] Trindade, F.C.L., Ferreira, T.S.D., Lopes, M.G., *et al.*: 'Mitigation of fast voltage variations during cloud transients in distribution systems with PV solar farms', *IEEE Trans. Power Del.*, 2017, **32**, pp. 921–932

[8] 'Reference technical rules for connecting active and passive users to the LV electricity utilities', CEI 0– 21:2011–12, Comitato Elettrotechnico Italiano, Milano, Italy, (2011).

[9] 'Negotiated customer connection contract (without construction, with generator embedded within customer network)'. Available at https://www.gci.uq.edu.au.

[10] Varma, R.K., Rahman, S.A., Vanderheide, T.: 'New control of PV solar farm as STATCOM (PV-STATCOM) for increasing grid power transmission limits during night and day', *IEEE Trans. Power Del.*, 2015, **30**, pp. 755–763

[11] Farivar, M., Neal, R., Clarke, C., *et al.*: 'Optimal inverter VAR control in distribution systems with high PV penetration', in proc. IEEE Power Energy Soc. Gener. Meet., San Diego, CA, USA, 22-26 July 2012.

[12] Xu, Y., Dong, Z.Y., Zhang, R., *et al.*: 'Multi-timescale coordinated voltage/Var control of high renewable-penetrated distribution systems', *IEEE Trans. Power Syst.*, 2017, **32**, pp. 4398–4408

[13] Samadi Eriksson, R., Söder, L., *et al.*: 'Coordinated active power-dependent voltage regulation in distribution grids with PV systems', *IEEE Trans. Power Del.*, 2014, **29**, pp. 1454–1464

[14] Demirok, E., González, P.C., Frederiksen, K.H.B., *et al.*: 'Local reactive power control methods for overvoltage prevention of distributed solar inverters in low-voltage grids', *IEEE Journ. Photovolt.*, 2011, **1**, pp. 174–182

[15] Zhang, Z., Ochoa, L.F., Valverde, G.: 'A novel voltage sensitivity approach for the decentralized control of DG plants', *IEEE Trans. Power Syst.*, 2018, **33**, pp. 1566–1576

[16] Zhu, H., Liu, H.J.: 'Fast local voltage control under limited reactive power: optimality and stability analysis', *IEEE Trans. Power Syst.*, 2016, **31**, pp. 3794–3803

[17] Baran, M.E., Wu, F.F.: 'Network reconfiguration in distribution systems for loss reduction and load balancing', *IEEE Trans. Power Del.*, 1989, **4**, pp. 1401–1407

[18] ‘B. Seal, BStandard language protocols for photovoltaics and storage grid integration’, EPRI 1020906. Available at http://my.epri.com/portal/server.pt?Abstract_id=000000000001020906

[19] eGauge502 Center: Available at http://egauge502.egaug.es/.

[20] Oahu solar measurement grid [Online]. Available at http://www.nrel.gov/midc/oahu_archive/.

[21] Akhavan-Rezai, E., Shaaban, M.F., El-Saadany, E.F., *et al.*: ‘Managing demand for plug-in electric vehicles in unbalanced LV systems with photovoltaics’, *IEEE Trans. Ind. Informat.*, 2017, **13**, pp. 1057–1067